J|A|C|S COMMUNICATIONS

Published on Web 04/07/2010

Tuning MOF CO_2 Adsorption Properties via Cation Exchange

Jihyun An and Nathaniel L. Rosi*

Department of Chemistry, University of Pittsburgh, 219 Parkman Avenue, Pittsburgh, Pennsylvania 15260

Received February 15, 2010; E-mail: nrosi@pitt.edu

Developing new materials for CO_2 capture and separation is critically important. Metal−organic frameworks (MOFs)[1] are emerging as promising materials for selectively adsorbing CO_2. In general, most research efforts in this area have focused on either (1) increasing the MOF pore volume and surface area to increase CO_2 capacity[2] or (2) modifying the pore chemistry by incorporating functional moieties having high affinities for CO_2.[3] Little experimental effort has focused on determining the optimal pore size for effectively condensing and adsorbing CO_2 at temperatures relevant to real-world application.

We have recently shown that metal−adeninate porous materials selectively capture large quantities of CO_2.[4] We attribute their favorable CO_2 adsorption properties to both the presence of adeninate amino and pyrimidine Lewis basic sites that decorate the pores and their relatively narrow pore dimensions. Given that these materials have exceptional capacities for CO_2 despite their relatively small and constricted pores, we decided to systematically evaluate the impact that pore volume has on a MOF's capacity for CO_2 adsorption.

To optimize a MOF for a particular application, it is important to be able to tailor its pore metrics and functionality in a straightforward fashion.[5] Postsynthetic MOF modification[6] has emerged as a facile means of introducing new functional moieties into MOF pores. Here, we demonstrate that postsynthetic exchange of extra-framework cations within anionic bio-MOF-1[7] can be used as a means to systematically modify its pore dimensions and metrics. We effectively utilize this strategy to optimize its CO_2 adsorption properties.

Bio-MOF-1, $Zn_8(ad)_4(BPDC)_6O{\bullet}2Me_2NH_2$, is a permanently porous MOF with infinite zinc-adeninate columnar secondary building units (SBUs) which are interconnected along [100] and [010] via biphenyldicarboxylate (BPDC) linkers, resulting in a 3-D extended structure with large 1-D channels (Figure 1A,B).[7] Bio-MOF-1 is anionic and dimethylammonium (DMA) cations reside in its pores. We have shown that the DMA cations are mobile and that they can be easily replaced with other organic cations, including cationic drug molecules.[7] To tailor the pore dimensions and pore volume of bio-MOF-1, we selected a series of organic cations which are structurally and chemically similar to DMA but each different in size (Figure 1C). We expected that as the organic cation size increased, the pore volume and surface area of the cation-exchanged bio-MOF-1 would decrease. Accordingly, we introduced tetramethylammonium (TMA), tetraethylammonium (TEA), and tetrabutylammonium (TBA) via cation exchange into the pores to systematically decrease the pore volume and surface area of the material.

Cation exchange was performed by soaking samples of as-synthesized bio-MOF-1 (**a**) in a DMF solution of TMA, TEA, or TBA to generate TMA@bio-MOF-1 (**b**), TEA@bio-MOF-1 (**c**), or TBA@bio-MOF-1 (**d**), respectively. In each case, retention of bio-MOF-1 crystallinity was confirmed using powder X-ray diffraction (Figure 1D) and complete exchange of the DMA cations

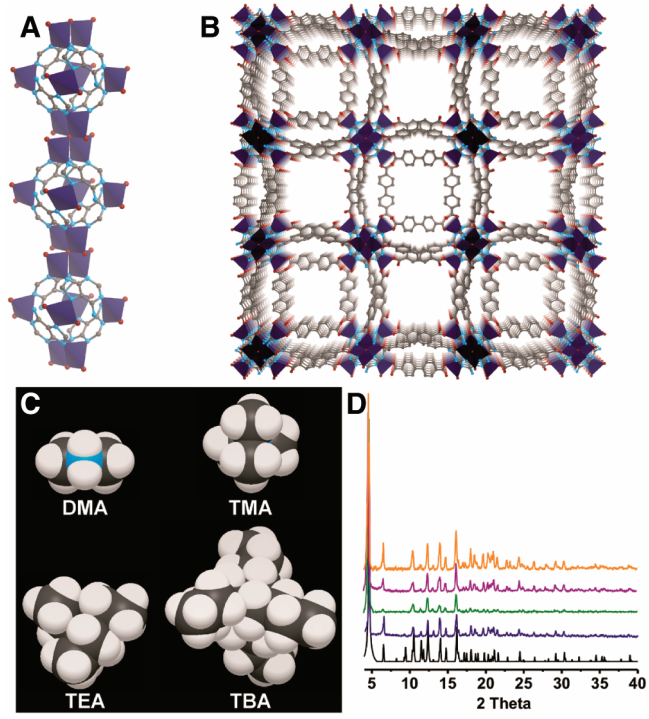

Figure 1. Bio-MOF-1 consists of zinc−adeninate columns (A) linked together by biphenyldicarboxylates into a 3-D crystal structure with 1-D pores (B) (Zn^{2+}, dark blue; C, dark gray; N, light blue; O, red; H omitted for clarity). (C) Space-filling representations of organic cations. (D) X-ray powder diffraction patterns for **a**−**d** (**a**, navy; **b**, green; **c**, purple; **d**, orange; simulated from single crystal X-ray data, black).

to yield [$Zn_8(Ad)_4(BPDC)_6O{\bullet}2$ cation] was determined using ^1H NMR and by correlating data from elemental and thermogravimetric analyses (see Supporting Information for details). To determine how the cation size impacts the pore volume and BET surface area, we collected N_2 adsorption isotherms for **a**−**d** (Figure 2A). Each material was activated at 100 °C under reduced pressure after soaking in chloroform for 24 h. The isotherms exhibited type-I behavior, were completely reversible, and showed no hysteresis upon desorption, which is consistent with permanent microporosity. Using this postsynthetic pore modification strategy, we were able to systematically decrease the pore volume and BET surface area from 0.75 cm^3/g and 1680 m^2/g for **a** to 0.37 cm^3/g and 830 m^2/g for **d** (Table 1).

To determine how these pore modifications would impact the CO_2 capacity of bio-MOF-1, we first studied the CO_2 adsorption of **a**−**d** at 273 K (Figure 2B). Interestingly, the CO_2 capacity of **a**−**d** did not scale with pore volume and BET surface area.[8] **b** adsorbed the largest amount of CO_2 (4.5 mmol/g at 1 bar), followed by **c** (4.2 mmol/g at 1 bar). The as-synthesized material, **a**, which has the largest BET surface area and pore volume, and **d**, which has the smallest BET surface area and pore volume, adsorbed 3.41

10.1021/ja1012992

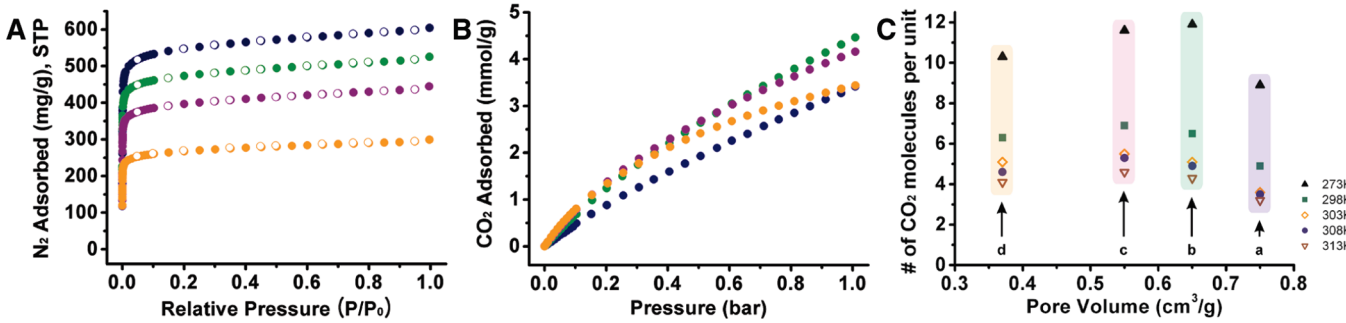

Figure 2. Gas adsorption experiments. (A) N_2 adsorption isotherms of **a**−**d** (77 K) and (B) CO_2 adsorption isotherms of **a**−**d** (273 K) (**a**, navy; **b**, green; **c**, purple; **d**, orange). (C) Number of CO_2 molecules adsorbed per formula unit ($Zn_8(Ad)_4(BPDC)_6O$•2 cation) versus pore volume of **a**−**d** at different adsorption temperatures (for isotherms: adsorption points, filled circles; desorption points, empty circles).

Table 1. N_2 and CO_2 Adsorption Data and Isosteric Heat of Adsorption Data for **a**−**d**

	BET SA[a]	V_p[b]	CO_2@273 K[c]	CO_2@313 K[c]	Q_{st}[d]
a	1680	0.75 (1951)	3.41 (8.91)	1.25 (3.25)	21.9
b	1460	0.65 (1732)	4.46 (11.9)	1.63 (4.34)	23.9
c	1220	0.55 (1528)	4.16 (11.6)	1.66 (4.62)	26.5
d	830	0.37 (1112)	3.44 (10.3)	1.36 (4.09)	31.2

[a] Surface area, m^2/g. [b] Pore volume, cm^3/g (cm^3/mol). [c] mmol/g (molecules CO_2/formula unit). [d] Isosteric heat of adsorption at 1 bar, kJ/mol.

mmol/g and 3.44 mmol/g CO_2, respectively, at 1 bar. We also calculated the number of CO_2 molecules adsorbed per formula unit ($Zn_8(Ad)_4(BPDC)_6O$•2 cation) for **a**−**d**. At 273 K, **b** and **c** adsorb 11.9 and 11.6 molecules of CO_2 per formula unit, respectively, while **a** and **d** adsorb 8.9 and 10.3 molecules of CO_2 per formula unit, respectively (Figure 2C; Table 1). From these data, we can conclude that pores with smaller volumes may be better suited for adsorbing CO_2, because **b**−**d** all adsorb more CO_2 per formula unit than **a**, even though they have smaller pore volumes.

We also collected CO_2 isotherms at higher temperatures (298, 303, 308, and 313 K; see Supporting Information) (Figure 2C; Table 1). In general, at these higher temperatures, the trend was similar to what was observed at 273 K. At all temperatures, **a** exhibited the lowest CO_2 capacity compared to **c**−**d**. **c** and **d** were comparatively more effective sorbents as the temperature increased. Specifically, we found that **c** had the largest CO_2 capacity at each of the elevated temperatures and **d** was nearly as effective as **b** at each of these temperatures. It is notable that **d** is a more effective CO_2 sorbent than **a** even though its pore volume and surface area are approximately half as large.

To better understand these observations, we calculated the isosteric heats of adsorption (Q_{st}) for **a**−**d** using the adsorption data collected at 298, 303, 308, and 313 K (see Supporting Information). The results of these experiments are consistent with the CO_2 uptake data. At zero loading, Q_{st} for **a**−**c** are each approximately 35 kJ/mol, while the initial Q_{st} for **d** is significantly larger, ∼55 kJ/mol. Q_{st} for **a**−**d** then decrease to constant values at higher CO_2 pressures (**a**, ∼22 kJ/mol; **b**, ∼24 kJ/mol; **c**, ∼26 kJ/mol; **d**, ∼31 kJ/mol) (Table 1). While **d** has the largest Q_{st}, its smaller pore volume may ultimately limit its CO_2 capacity. These data suggest that smaller pores lead to stronger adsorbate/sorbent interactions.

In summary, we showed that the pore size of bio-MOF-1 can be modified postsynthetically via straightforward cation-exchange experiments and that such modifications can be used to systematically tune the CO_2 adsorption capacity of this material. From our data, we can conclude that smaller pores in MOFs may be ideal for condensing CO_2 at temperatures relevant to real-world application.[9]

Acknowledgment. Funding for this work was provided by the University of Pittsburgh and the American Chemical Society Petroleum Research Fund (PRF 47601-G10). The authors thank the Petersen Institute for Nanoscience and Engineering for access to XRPD instrumentation.

Supporting Information Available: Experimental procedures and additional supporting data. This material is available free of charge via the Internet at http://pubs.acs.org.

References

(1) (a) Rowsell, J. L. C.; Yaghi, O. M. *Microporous Mesoporous Mater.* **2004**, *73*, 3. (b) Kitagawa, S.; Kitaura, R.; Noro, S. *Angew. Chem., Int. Ed.* **2004**, *43*, 2334. (c) Ferey, G. *Chem. Soc. Rev.* **2008**, *37*, 191. (d) Li, J. R.; Kuppler, R. J.; Zhou, H. C. *Chem. Soc. Rev.* **2009**, *38*, 1477.

(2) (a) Millward, A. R.; Yaghi, O. M. *J. Am. Chem. Soc.* **2005**, *127*, 17998. (b) Llewellyn, P. L.; Bourrelly, S.; Serre, C.; Vimont, A.; Daturi, M.; Hamon, L.; De Weireld, G.; Chang, J. S.; Hong, D. Y.; Hwang, Y. K.; Jhung, S. H.; Ferey, G. *Langmuir* **2008**, *24*, 7245.

(3) (a) Caskey, S. R.; Wong-Foy, A. G.; Matzger, A. J. *J. Am. Chem. Soc.* **2008**, *130*, 10870. (b) Demessence, A.; D'Alessandro, D. M.; Foo, M. L.; Long, J. R. *J. Am. Chem. Soc.* **2009**, *131*, 8784. (c) Bae, Y. S.; Farha, O. K.; Hupp, J. T.; Snurr, R. Q. *J. Mater. Chem.* **2009**, *19*, 2131. (d) Arstad, B.; Fjellvag, H.; Kongshaug, K. O.; Swang, O.; Blom, R. *Adsorption* **2008**, *14*, 755. (e) Banerjee, R.; Furukawa, H.; Britt, D.; Knobler, C.; O'Keeffe, M.; Yaghi, O. M. *J. Am. Chem. Soc.* **2009**, *131*, 3875. (f) Vaidhyanathan, R.; Iremonger, S. S.; Dawson, K. W.; Shimizu, G. K. H. *Chem. Commun.* **2009**, 5230. (g) Chen, S. M.; Zhang, J.; Wu, T.; Feng, P. Y.; Bu, X. H. *J. Am. Chem. Soc.* **2009**, *131*, 16027.

(4) (a) An, J.; Fiorella, R.; Geib, S. J.; Rosi, N. L. *J. Am. Chem. Soc.* **2009**, *131*, 8401. (b) An, J.; Geib, S. J.; Rosi, N. L. *J. Am. Chem. Soc.* **2010**, *132*, 38.

(5) Eddaoudi, M.; Kim, J.; Rosi, N.; Vodak, D.; Wachter, J.; O'Keefe, M.; Yaghi, O. M. *Science* **2002**, *295*, 469.

(6) Wang, Z. Q.; Cohen, S. M. *Chem. Soc. Rev.* **2009**, *38*, 1315, and references therein.

(7) An, J.; Geib, S. J.; Rosi, N. L. *J. Am. Chem. Soc.* **2009**, *131*, 8376.

(8) Frost, H.; Duren, T.; Snurr, R. Q. *J. Phys. Chem. B* **2006**, *110*, 9565.

(9) Pennline, H. W.; Luebke, D. R.; Jones, K. L.; Myers, C. R.; Morsi, B. I.; Heintz, Y. J.; Ilconich, J. B. *Fuel Process. Technol.* **2008**, *89*, 897.

JA1012992